ADVANCED FUNCTIONAL MATERIALS

www.afm-journal.de

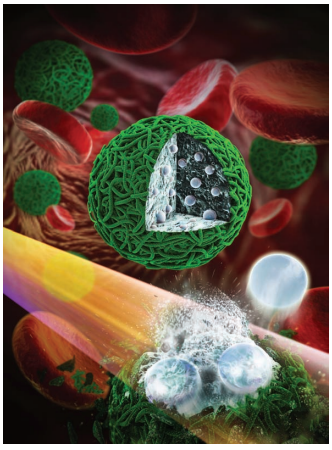

Biomedical Applications

On page 5518, an ultralong-acting, liver-specific, ultrasound contrast agent is presented in the form of self-assembled, echogenic hyaluronic acid nanoparticles. I. C. Kwon, K. Kim, and co-workers use hydrophobic interactions and an oil-in-water emulsification method to encapsulate bioinert and hydrophobic perfluoropentane as an ultrasound gas precursor into the nanoparticles. These particles are more stable and robust echogenic solid bodies than the conventional microbubbles, with an in vivo favorable hydrodynamic size.

Li-Ion Batteries

A microscopic model for voltage suppression in complex transition metal oxides is proposed by M. L. Sushko and co-workers based on careful analysis of the electronic structure and electrostatic potential in one of the most promising cathode materials—$LiNi_{0.5}Mn_{1.5}O_4$—as a case study. On page 5530, ab initio simulations reveal that the electrochemical performance of $LiNi_{0.5}Mn_{1.5}O_4$ and similar transition metal oxides can be finely tuned by controlling the concentration of oxygen vacancies.

Nanoparticles

Electrochemical dealloying and confinement effects are combined by J. Erlebacher and co-workers in order to produce nanoporous proton exchange membrane fuel cells with both a high surface area and enhanced oxygen reduction reaction catalysis. On page 5494, they incorporate a hydrophobic, protic ionic liquid into the pores of high surface-area NiPt alloy nanoparticles (np-NiPt/C + [MTBD][beti]). The high O_2 solubility of the [MTBD][beti], in conjunction with the confined environment within the pores, bias the reactant O_2 toward the catalytic surface.

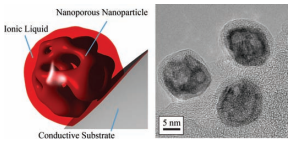

CONTENTS

FEATURE ARTICLE

Tissue Engineering

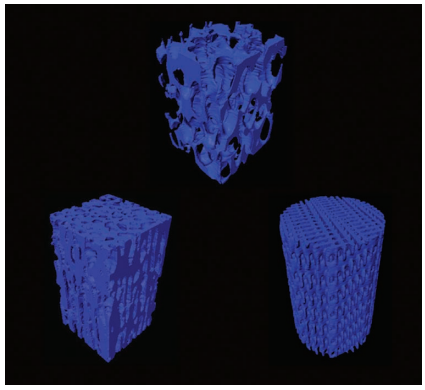

Fundamental understanding of the processing-structure-property relationships of porous glass and ceramic scaffolds is critical for the creation of strong and tough implants. Recent developments in the use of design principles and novel fabrication technologies are paving the way to the fabrication of synthetic scaffolds of isotropic, anisotropic, and periodic architectures with promising potential for bone repair.

FULL PAPERS

Thermoelectrics

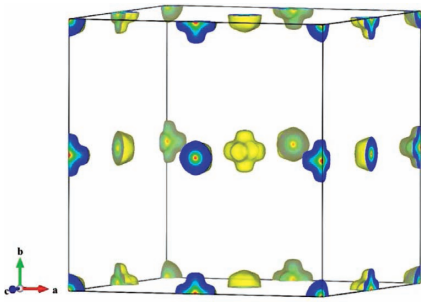

Analysis of synchrotron powder X-ray diffraction data provides detailed insight into the atomic disorder responsible for the extraordinary low thermal conductivities in the thermoelectric lead chalcogenides PbTe and PbS.

Polymers

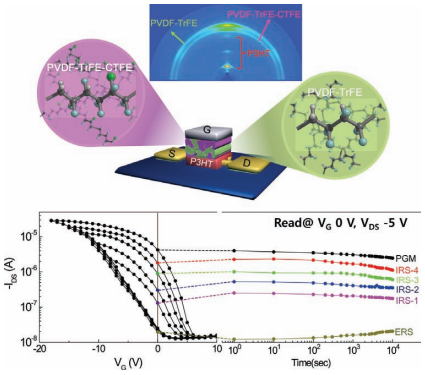

Low voltage operation of a polymer ferroelectric field effect transistor memory with multilevel data storage states is realized with a high dielectric constant (*k*) ferroelectric gate insulator based on simple binary solution blending of a ferroelectric poly(vinylidene fluoride-co-trifluoroethylene) and a relaxer high-*k* poly(vinylidene-fluoride–trifluoroethylene–chlorotrifluoroethylene). The device shows discrete six-level multi-state operation with excellent data retention and endurance of each state.

Nanoparticles

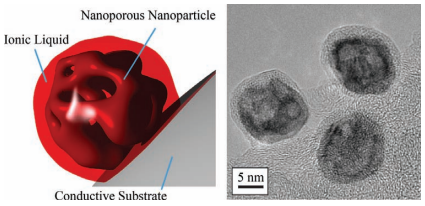

Nanoporous Ni/Pt nanoparticles exhibit mass activities nearly an order of magnitude higher than Pt/C when encapsulated with [MTBD][beti] ionic liquids, both in half-cell measurements and fuel cell testing.

FULL PAPERS

Although carbon nanotube forests are synonymous with optical opaqueness, the growth of up to 20 µm tall forests is shown, featuring optical transparency in the visible and infrared light ranges. Additionally, they are grown on heat-sensitive substrates below 300 °C, opening prospects for carbon optoelectronics. It is shown that transparency occurs in the visible light range by light channelling through subwavelength voids in the forests, acting as waveguides.

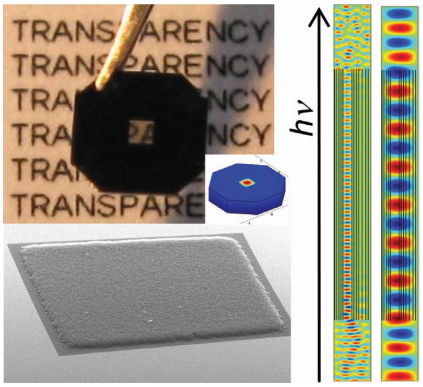

Carbon Nanotubes

A few-layer WS2 photosensor shows variations in the conduction current by switching a laser on and off. An extensive study reveals that few-layered WS_2 grown by CVD can be used as an efficient light sensor in the visible spectral region for a wide range of incident intensities with a fast response in the order of a few milliseconds (e.g., 5.3 ms).

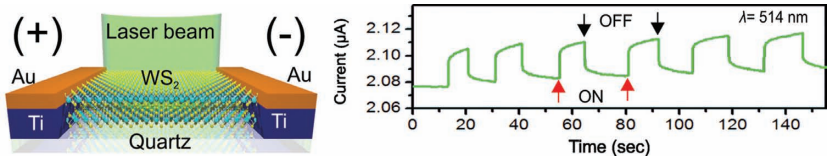

Sensors

A new species of echogenic hyaluronic acid (HA) nanoparticles is presented as an ultralong-acting, liver-specific, ultrasound contrast agent (UCA) that is distinct from conventional gas-filled microbubbles. The approach of utilizing preformulated solid nanoparticles as templates to load liquid gas precursors provides advantages in the construction of a long-acting UCAs and greatly improved echogenic properties are observed.

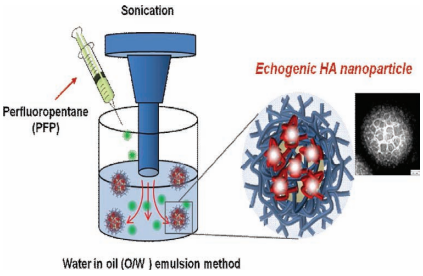

Biomedical Applications

The complex correlation between the structure of oxygen deficient spinel $LiNi_{0.5}Mn_{1.5}O_{4-\delta}$ and its ion and electron transport properties is revealed through first principles simulations. It is shown that neutral oxygen vacancies promote cation disorder leading to the creation of deep and shallow Mn^{3+} states, responsible for high and low voltage regions on the voltage–capacity curves.

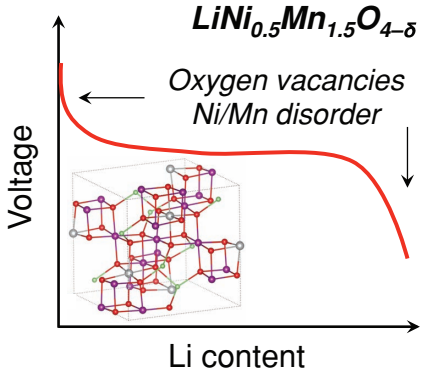

Li-Ion Batteries

CONTENTS

FULL PAPERS

Nanocomposites

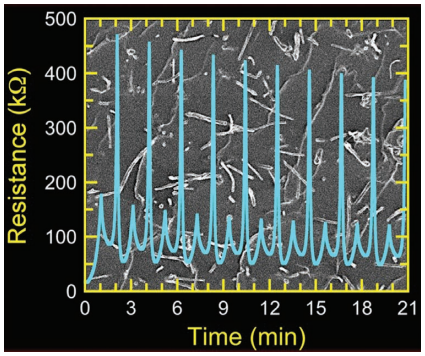

The incorporation of carbon nanofibers into plasticized poly(vinyl chloride) (PVC) or poly(dimethylsiloxane) (PDMS) elastomers yields conductive nanocomposites that can be printed on fabrics to produce electronic textiles (e.g., strain sensors). Upon strain cycling, the nanofibers undergo reorientation and subsequent separation, causing the nanocomposites to exhibit strain-reversible piezoresistivity.

Microfluidics

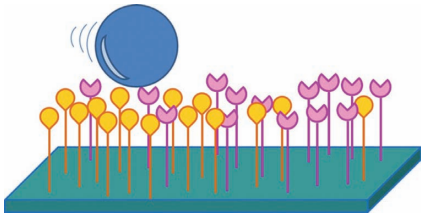

A simple and versatile procedure, based on the immersion method, is developed to fabricate chemical gradients on Si/SiO_2 surfaces by using a silane self-assembly monolayer. The spontaneous motion of water droplet is demonstrated and the results are rationalized by dissipative particle dynamics simulations that show that the intrinsic nature of the gradient affects the velocity of the motion.

Light-Emitting Diodes

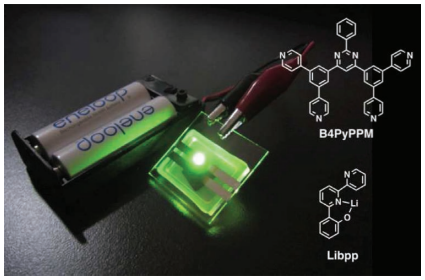

Green phosphorescent organic light-emitting diodes (OLEDs) operating below a theoretical limit of the energy gap voltage with high external quantum efficiency over 20% are developed. An optimized OLED operates clearly below the energy gap voltage of 2.38 V showing 100 cd m^{-2} at 2.25 V and 5000 cd m^{-2} at 2.95 V without any light outcoupling enhancement techniques.

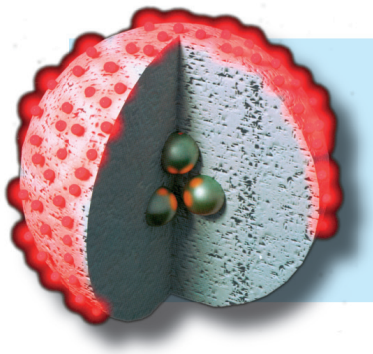

How to contact us:

Editorial Office:
Phone: (+49) 6201-606-286/531
Fax: (+49) 6201-606-500
Email: afm@wiley-vch.de

Reprints:
cherth@wiley-vch.de

Copyright Permission:
Fax: (+49) 6201-606-332
Email: rights@wiley-vch.de

The effect of varying the material forming the back electrode in a protein-based photoelectrochemical cell that produces an alternating current under discontinuous illumination is explored. A near-symmetrical alternating current is obtained by constructing a bio-hybrid cell in which this back electrode is formed from a layer of superhydrophobic multi-walled carbon nanotubes.

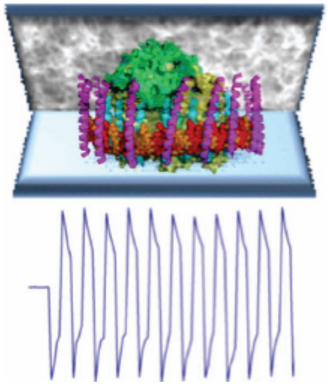

Photovoltaics